ELSEVIER

Chemical Engineering Journal 86 (2002) 95–101

Chemical Engineering Journal

www.elsevier.com/locate/cej

Influence of the mechanical behavior law on the drying of an alumina gel

Frédéric Mercier [a,*], Frédéric Kolenda [b], Jean Rodolphe Puiggali [c]

[a] *CENERG ENSMP, 60 Bd St Michel, 75272 Paris, France*
[b] *IFP CEDI, echangeur Solaize, 69360 Solaize, France*
[c] *LEPT ENSAM, Esplanade des Arts et Métiers, 33400 Talence, France*

Abstract

Some catalysts supports are made from gelified alumina pellets. In the manufacturing process, drying can be an important stage in improving both texture and strength. In order to ease the comprehension of the phenomena, the drying of a pellet has been modeled with an Eulerian set of conservation equations (mass, energy and motion). A pseudo-elastic law issued from rheological experiments has been used to close the mechanical problem. © 2002 Published by Elsevier Science B.V.

Keywords: Alumina; Coupled transport; Gel; Modeling; Rheology; Shrinkage

1. Introduction

Aluminas are widely used in the chemical industry. In catalyst reforming, the synthesis of catalysts supports uses a colloidal sol–gel route. The catalysts supports studied in the present work are prepared following the flowchart of Fig. 1. In the first step, the suspension of a colloidal powder is formed by mechanical dispersion of a microcrystalline powder of boehmite in an aqueous solution of nitric acid. The ensuing material is a gelatinous precipitate whose peptization rouses a light charging of the boehmite platelets in order to ease the shaping, that occurs in the second step: gelation. By oil dropping the latter precipitate in a basic solution, colloidal particles link together, so that they form a three-dimensional network. The shape and size of the gelified beads are linked to the diameter of the dropping needle. In the third step, drying in air performs the transition of the gel to a solid, an aerogel. Since the support has to be acidic in order to activate isomerization and dehydrocyclization reactions, it is then fired at 600 °C in an atmospheric furnace to lose its structural water and become a γ-alumina support.

During the reforming process, the catalyst works as a molecular traps and suffers from hard thermomechanical conditions that may involve damages. One of the stake of the supports manufacturing is to better both their resistance and their pores range. As a stage where the mean diameter of the pellets drops from 4 to 2 mm and at the same time the porosity becomes visible, drying appears to be a favorable phase to reach these aims.

The improvement of the comprehension of the drying processes needs a model that describes both the heat and mass transfer and the deformation of a drying pellet.

2. Experimental

2.1. Physical properties of the pellets

Table 1 gives the physical properties of the pellets. The stoichiometric composition is determined by firing the beads up to their transformation into α-alumina, the metastable alumina. The initial solvent content is measured after heating the beads at 120 °C during 24 h. Specific surface is evaluated with BET. Pores size is determined using mercury porometry [1].

2.2. Sorption curves

Sorption curves are determined by the isopieztic method (Fig. 2). They present a very short monolayer zone and a very long multilayer zone. The third zone begins for water activity around 0.5. The main characteristic of these curves is that the solvent in zone 3 is quasi-exclusively composed of bound microcapillary liquid, as set off from the typical flat-shaped curves for high activities. Their fit using a the Guggenheim, Anderson and de Boer (GAB) model appears to be the most appropriate for this product, since the monolayer surface computed from this model has a similar value to the one issued from BET (approximately 220 m^2/g) (Table 2).

$$W_{eq} = \frac{W_{mono} a_w LM}{(1 - a_w M)(1 + a_w LM - a_w M)} \quad (1)$$

* Corresponding author. Tel.: +33-1-40-51-91-56; fax: +33-1-46-34-24-91.
E-mail address: frederic.mercier@cenerg.ensmp.fr (F. Mercier).

1385-8947/02/$ – see front matter © 2002 Published by Elsevier Science B.V.
PII: S1385-8947(01)00277-7

Nomenclature

a	activity (–)
C	massic fraction (–)
C_p	specific heat (J/kg K)
D	transport coefficient (m^2/s)
F	mass flux (kg/m^2 s)
G	relaxation modulus (Pa)
h	external transfer coefficient (m/s)
Δhv	vaporization enthalpy (J/kg)
K	bulk modulus (kg/m^2 s)
L	coefficient of GAB fit (–)
M	coefficient of GAB fit (–)
RH	relative humidity (–)
T	temperature (°C)
u	displacement vector (m)
v	velocity vector (m/s)

Greek symbols

δ	Kronecker symbol (–)
ε	strain tensor
λ	thermal conductivity
μ	second Lamé coefficient (Pa)
ν	Poisson ratio (Pa)
ρ	volumetric concentration (kg/m^3)
σ	stress tensor (Pa)

Superscripts

g	gas phase
l	liquid phase
s	solid phase
0	dry
overline	local volume averaged quantity

Subscripts

anh	anhydrous
eff	bound moisture
eq	equilibrium
l	liquid phase
m	material
mono	monolayer
s	solid phase
∞	ambiance

Table 1
Physical properties of boehmite pellet

Stoichiometric composition	$Al_2O_3 \cdot 1.87H_2O$
Solvent content (d.b.)	3.5
Specific surface (m^2/g)	276
Porous distribution	Monomodal at 47 Å
Specific porous volume (cm^2/g)	0.365

2.3. Shrinkage curves

Drying triggers a very important reduction since the volume of the dry pellet is the eighth of the initial volume. Specific shrinkage curves result from photography survey (Fig. 3). They depict an ideal contraction for moisture content down to 1, whatever the air conditions (RH, T). During this step, the volume change is directly bound to the water removal. So following Kneule [2], no textural change is supposed to happen until moisture contents lowers approximately 1.

2.4. Rheology

The rheology of wet samples has been studied on an imposed shear stress plate–plate rheometer. Rheometric study of dry samples has been conducted on both an imposed strain rheometer and an ultrasonic device in order to check the accordance between the results. The moisture contents between 1 and 0 have not been investigated, since the applied stresses involve the desegregation of the product. The storage modulus as well as the loss modulus versus the frequency are plateau-like curves, which is typical of a gel (Fig. 4). Both moduli are increasing with lower moisture contents, which is normal for the storage modulus but more unusual for the loss modulus: the viscous part of a gel becoming a solid should diminish (Fig. 5). In fact, it consists in the response of the particles part of the gel to the increasing stresses.

Table 2
Identified GAB model coefficients for the boehmite beads

Temperature (°C)	W_{mono}	L	M
30	0.08	20.52	0.906
50	0.06	14.00	0.92
70	0.045	13.00	0.945
82	0.032	10.00	0.97

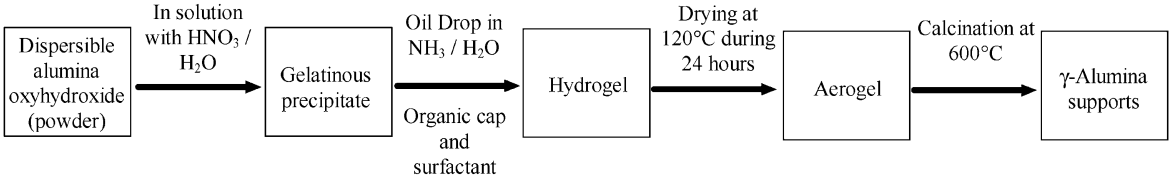

Fig. 1. Flowchart of the supports synthesis.

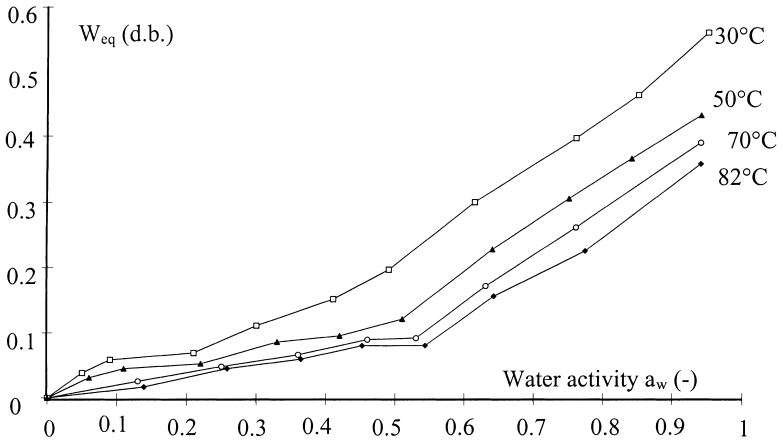

Fig. 2. Sorption curves.

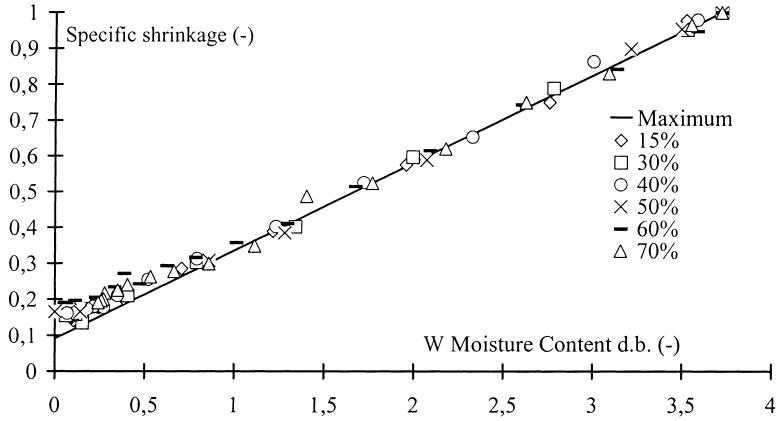

Fig. 3. Shrinkage curves for different RH.

We finally adopt a pseudo-elastic deformation model in which the bulk modulus K and the second Lamé coefficient are function of the moisture content

$$\sigma_{ij} = (K(W) - \tfrac{2}{3}\mu(W))\varepsilon^*_{kk}\delta_{ij} + 2\mu(W)\varepsilon^*_{ij} \quad (2)$$

where the bulk modulus results from G by the following equation:

$$K = \frac{2(1+\nu)}{3(1-2\nu)}G \quad (3)$$

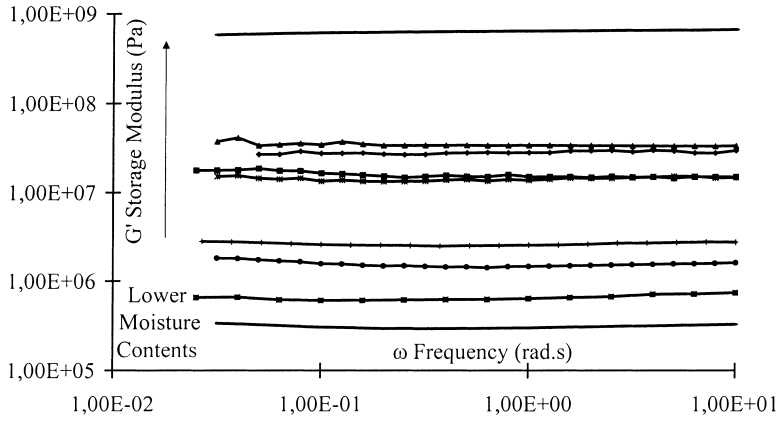

Fig. 4. Storage moduli vs. frequency.

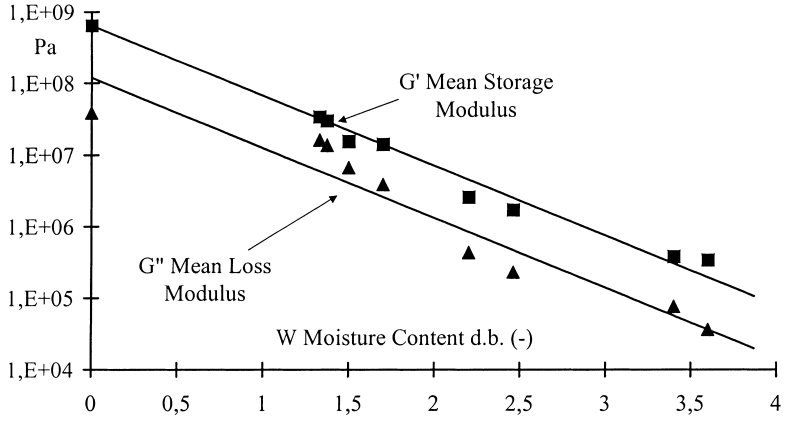

Fig. 5. Mean loss and storage moduli vs. *W*.

2.5. Specific heat of the gel

The specific heat of a dry sample has been measured on a Dynamic Scan Calorimeter. It has been correlated as follows:

$$C_{p\,\mathrm{anh}} = a + b(T-273) + c(T-273)^{1.5} + d(T-273)^2 + e(T-273)^{2.5} \quad (4)$$

where T is the absolute temperature (K) and

$$a = 784.94, \quad b = 14.36, \quad c = -4.11, \quad d = 0.59, \quad e = -0.03 \quad (5)$$

We have then assumed that the specific heat of the gel verifies a barycentric relation (Fig. 6)

$$C_{p\,\mathrm{gel}}(W) = \left(\frac{W}{1+W}\right) C_{p\,\mathrm{w}} + \left(\frac{1}{1+W}\right) C_{p\,\mathrm{anh}} \quad (6)$$

2.6. Transport coefficient

Due to the fact that the pore size of the gel is of the order of some nanometers, we suppose that the transport of the solvent conforms to Fick's law [3].

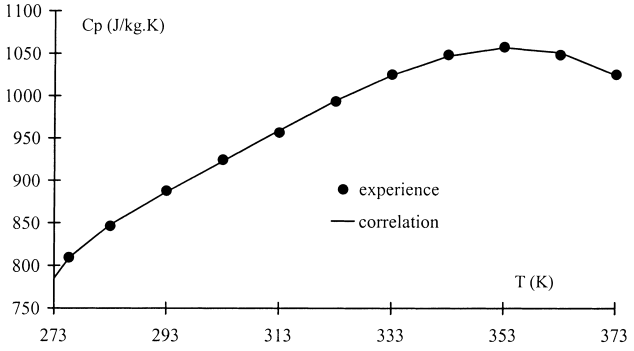

Fig. 6. Specific heat vs. absolute temperature of an anhydrous gel sample.

Crank [4] expressed the diffusion of solvent in a non-shrinking sphere (viz. in Lagrangian coordinates) as

$$\frac{F_{\mathrm{m}}(t)}{\int_{t=0}^{\infty} F_{\mathrm{m}}(\tau)\,\mathrm{d}\tau} = 1 - \frac{6}{\pi^2}\sum_{n=1}^{\infty}\frac{1}{n^2}\exp\left(-\frac{D_{\mathrm{eff}} n^2 \pi^2 t}{R^2}\right) \quad (7)$$

Since the exponential is decreasing very quickly, it is possible to identify D_{eff} from the following:

$$D_{\mathrm{eff}} = -\frac{R^2}{\pi^2 t}\ln\left(\left(1 - \frac{F_{\mathrm{m}}(t)}{\int_{t=0}^{\infty} F_{\mathrm{m}}(t)\,\mathrm{d}\tau}\right)\frac{\pi^2}{6}\right) \quad (8)$$

From D_{eff}, the Eulerian transport coefficient D_{m} can be written as

$$D_{\mathrm{m}} = D_{\mathrm{eff}}\left(\frac{\rho_{\mathrm{s}}}{\rho_{\mathrm{s}}^0}\right)^{2/3} \quad (9)$$

3. Model of a drying pellet

3.1. Constitutive equations

The model described thereafter is an extension of a model developed by Jomaa and Puigalli [5]. The pellet is assumed to be a shrinking medium in which the liquid and solid phases are followed during the drying. All the set of equations is written in Eulerian coordinates, so that mechanical behavior law can be injected in the model by the mean of the solid velocity.

- Motion equations

$$\tilde{\nabla} \cdot \langle \underset{\approx}{\sigma}_{\mathrm{s}} \rangle = 0 \quad (10)$$

with a boundary condition that expresses the lack of load at the surface of the pellet

$$\langle \underset{\approx}{\sigma}_{\mathrm{s}} \rangle \cdot \tilde{n}_{\mathrm{surf}} = 0 \quad (11)$$

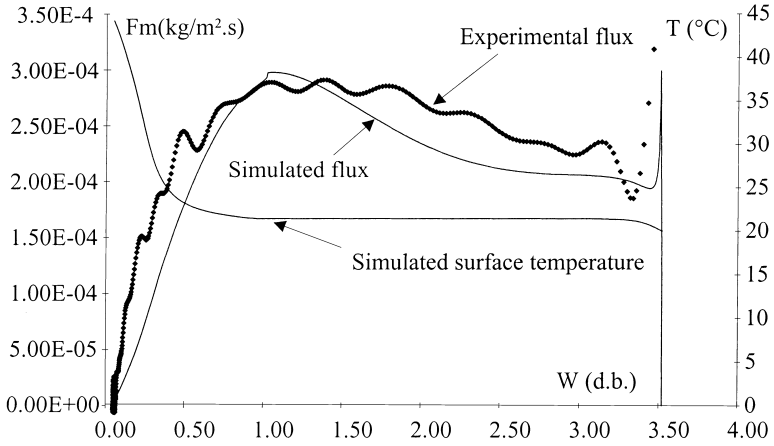

Fig. 7. Comparison between experiment and simulation on mass flow.

- Continuity equation

$$\frac{\partial}{\partial t}\langle\rho_l\rangle + \tilde{\nabla}\cdot(\langle\rho_l\rangle\langle\tilde{v}_s\rangle^s) = \tilde{\nabla}\cdot(D_m\,\tilde{\nabla}\langle\rho_l\rangle) \quad (12)$$

with a boundary condition on the continuity of the mass flow at the interface of the pellet and the air

$$F_m = -D_m\,\tilde{\nabla}\langle\rho_l\rangle\cdot\tilde{n}_{surf} = h_c(C_{surf} - C_\infty) \quad (13)$$

- Energy equation

$$(\rho C_p)\frac{\partial\langle T\rangle}{\partial t} + ((\rho C_p)\langle\tilde{v}_s\rangle^s - C_p^l D_m\,\tilde{\nabla}\langle\rho_l\rangle)\tilde{\nabla}\langle T\rangle = \tilde{\nabla}\cdot(\underset{\approx}{\lambda}\,\tilde{\nabla}\langle T\rangle) + \langle\Phi\rangle \quad (14)$$

with a boundary condition on the continuity of the heat flow at the interface of the pellet and the air

$$\varphi(\underset{\approx}{\lambda}\,\tilde{\nabla}\langle T\rangle)\cdot\tilde{n}_{surf} = F_m\,\Delta H_v(T_{surf}) + h_T(T_{surf} - T_\infty) \quad (15)$$

3.2. The rheological problem

The strain tensor results from the solid displacement by

$$\underset{\approx}{\varepsilon}^s = \tfrac{1}{2}({}^t\tilde{\nabla}\tilde{u}^s + \tilde{\nabla}\tilde{u}^s + {}^t\tilde{\nabla}\tilde{u}^s\cdot\tilde{\nabla}\tilde{u}^s) \cong \tfrac{1}{2}({}^t\tilde{\nabla}\tilde{u}^s + \tilde{\nabla}\tilde{u}^s) \quad (16)$$

and the solid velocity and the displacement are relied by

$$\langle\tilde{v}_s\rangle^s = \frac{\partial\tilde{u}^s}{\partial t} \quad (17)$$

The strain tensor can be discomposed into a part resulting from the behavior of the material ε^* and an other part coming from both hydric and thermal expansions ε^r [6]:

$$\underset{\approx}{\varepsilon} = \underset{\approx}{\varepsilon}^* + \underset{\approx}{\varepsilon}^r \quad (18)$$

Thus minimizing the following variational formalism leads to the solution of Eq. (10):

$$V = \frac{1}{2}\int_\Omega \left(\left(K - \frac{2}{3}\mu\right)(\varepsilon_{ij} - \varepsilon_{ij}^r)\delta_{ij} + 2\mu(\varepsilon_{ij} - \varepsilon_{ij}^r)\right)\varepsilon_{ij}\,d\Omega \quad (19)$$

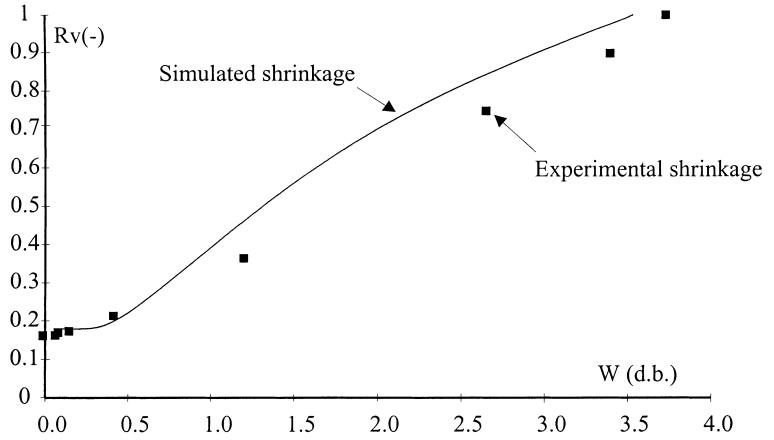

Fig. 8. Comparison between experiment and simulation on specific shrinkage.

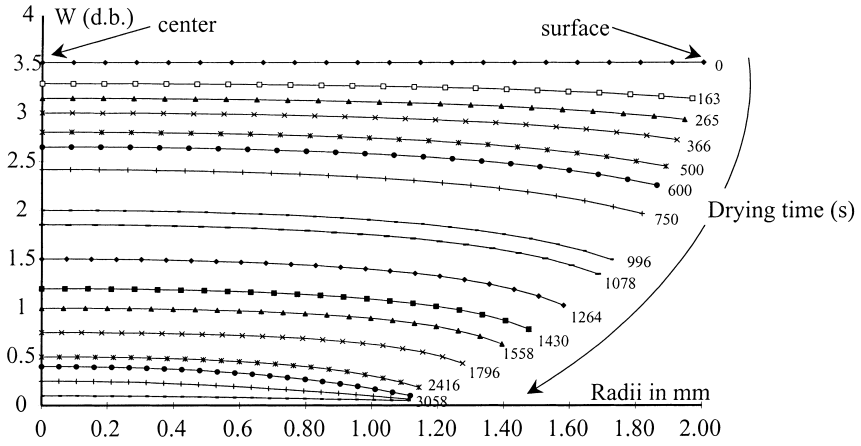

Fig. 9. Simulated moisture content fields evolution with drying.

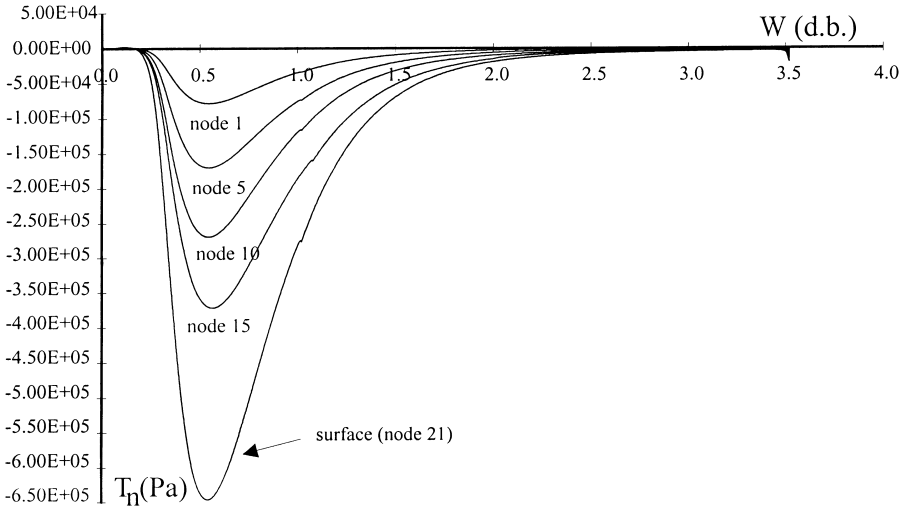

Fig. 10. Simulated normal stresses evolution during drying.

where K and μ are moisture content dependent, as found in the rheology survey.

To solve the whole problem, we have chosen to solve separately each system by using spherical piecewise finite elements for Eq. (19) [7] and spherical finite differences for the others. Since it is a moving boundary problem, it is necessary to re-mesh the domain after each minimization of Eq. (19).

4. Results and discussion

The simulation is in a good agreement with the experiment as pictured in Fig. 7. Experimental mass flux shows a long pseudo-isenthalpic plateau from the starting moisture content down to an average moisture content neighboring 1, which corresponds locally to the beginning of the hygroscopic domain. The simulated mass flux presents this characteristic plateau as well, in an order of value similar to the one of the experimental mass flux. The simulated temperature is coherent with experimental observations [1] that indicate that the material remains at the wet bulb temperature during the pseudo-isenthalpic stage before rising up to the dry temperature at the end of drying.

However the model is a bit less efficient to describe the specific shrinkage (Fig. 8). Simulated moisture content fields as well as the pellet radius are pictured in Fig. 9. The flat shape of the moisture content fields results from a strong mass transport.

Normal stresses evolution during drying is plotted in Fig. 10. The maximum stress is reached at the surface node. But the most important information is that the range [0.4, 1] in moisture content is a critical period for the drying of the pellets. As an example, they can be damaged by internal stresses.

5. Conclusions

A two phases model for the drying of alumina pellet has been written. Its mechanical closure results from a

pseudo-elastic law where the coefficients are identified from a rheometric survey on wet and dry samples. With this model, simulations present a good agreement with experiment. One of the result is the evidence that the stage of drying when moisture contents comprised between 0.4 and 1 is critical for the material.

Acknowledgements

This study is part of a Ph.D. work [1] sponsored by the Institut Français du Pétrole (France).

References

[1] F. Mercier, Drying of alumina gel: mastering the texture of catalysts supports, Ph.D. Thesis, Energy Studies, Pau University, 1996 (in French).

[2] F. Kneule, Le séchage (dasTrocknen), Éditions Eyrolles, Paris, 1964.

[3] J.R. Puiggali, M. Quintard, S. Whitaker, Drying granular porous media: gravitational effects and the role of diffusion models, Drying Technol. 6 (4) (1988) 601–629.

[4] J. Crank, The Mathematics of Diffusion, 2nd Edition, Clarendon Press, Oxford, 1979.

[5] W. Jomaa, J.R. Puigalli, Drying of shrinking materials: modellings with shrinkage velocity, Drying Technol. 9 (5) (1991) 1271–1293.

[6] Y. Itaya, S. Mabuchi, M. Hasatani, Deformation behavior of ceramic slabs by nonuniform drying, Drying Technol. 13 (3) (1995) 801–819.

[7] K. Haghighi, L.J. Segherlind, Failure of biomaterials subjected to temperature and moisture gradients using the finite element method. I. Thermo-hydro viscoelasticity, Trans. ASAE 31 (3) (1988) 930–937; K. Haghighi, L.J. Segherlind, Failure of biomaterials subjected to temperature and moisture gradients using the finite element method. II. Stress analysis of an isotropic sphere during drying, Trans. ASAE 31 (3) (1988) 938–946.